Nonisothermal Simulation of Flows in the Hot-Gas Filter Vessel at Wilsonville

ISAAC K. GAMWO
JOHN S. HALOW

United States Department of Energy
National Energy Technology Laboratory
Pittsburgh, Pennsylvania, USA

GOODARZ AHMADI

Department of Mechanical and Aeronautical Engineering
Clarkson University
Postdam, New York, USA

A numerical simulation of nonisothermal gas flows in the hot-gas filter vessel at the Power Systems Development Facility in Wilsonville, Alabama is presented. The gas velocity and thermal simulations are based on the Reynolds stress transport turbulence model of the FLUENT™ commercial CFD computer code. While earlier modeling studies were limited to isothermal conditions, in this study, the energy transport equation was solved in addition to the mass and momentum equations. The gas flow and temperature field inside the filter vessel were also studied. Results reveal that the gas flow shows strong rotating flow regions outside the shroud and in the upper and lower parts of the body of the vessel. It is also shown that the temperature distribution is nonuniform with somewhat higher temperatures in the upper part of the filter. The simulated results qualitatively agree with the experimental field observations of the filter vessel.

Keywords filter vessel, numerical simulation, nonisothermal, FLUENT

The authors would like to thank John Foote and Howard Hendrix, of Southern Company Services, Zal Sanjana of Siemens Westinghouse, Edward J. Boyle, Theodore McMahon, Richard Dennis, and Tom O'Brien for many helpful discussions on the filter vessel. Special thanks is given to Xiaofeng Guan for his in-depth review and constructive comments on this manuscript, and to Hiafeng Zhang and Richard Anderson for their assistance in the manuscript preparation. The authors would like to thank the reviewers for helpful comments. The work of G. Ahmadi was supported by the DOE grant DE-FC26-98T4047. Thanks is also given to FLUENT™ Corporation for making the code available.

Address correspondence to Isaac K. Gamwo, U.S. Department of Energy, National Energy Technology Laboratory, P.O. Box 10940, Pittsburgh, PA 15236-0940, USA. E-mail: gamwo@netl.doe.gov

Introduction

The development of clean coal technology for electric power generation is a major goal of the U.S. Department of Energy as well as the power industry. As a result, highly efficient advanced Pressurized Fluidized Bed Combustors (PFBC) and Integrated Gasification Combined Cycle (IGCC) systems are being developed and tested. These advanced coal-fired systems require effective separation of fine particles from high-temperature, high-pressure gas streams produced from coal combustion and/or gasification. Effective removal of particulate matter from the hot gas is essential for protecting the downstream gas turbine components from damage due to fouling and erosion. In addition the gas needs to be cleaned to meet strict particulate emission requirements.

Currently the effort for hot-gas cleaning of advanced coal-fired energy systems is focused on the use of ceramic candle filters due to its high efficiency and capability to operate at high temperatures. Each candle filter has an inner diameter of about 6 cm, a length of 1 to 1.5 m, and a wall thickness of about 1 cm. An industrial unit normally contains a large number of candle filters. During the operation of the filter vessel, the clean hot gas passes through the porous walls of the ceramic filters. The ash particles form a deposit on the outside of the candle filter as a filter cake. As the filter cake builds up, the filter pressure drop increases. To avoid excessive pressure drop, groups of candle filters are periodically cleaned by a rapid backpulse procedure.

Under ideal operating conditions, the candle filters are periodically well cleaned, and the filtration system effectively removes fine particles and delivers essentially particulate-free hot gases that meet turbine engineering requirements and regulatory standards for power plant emissions (Lippert et al., 1995; Radiann, 1994). On occasion, ash deposits build up in the filter vessel and lead to a phenomenon called "filter bridging." This occurs when all of the space between adjacent filter surfaces has been filled by particles. This normally leads to disruption of the filtration process due to candle filter failure and/or excessive pressure drop. Smith and Ahmadi (1998) suggested, among other hypotheses, that "filter bridging" is caused by particles depositing on solid surfaces (tube sheets and central post) that have no cleaning mechanisms. In addition, the incomplete filter cleaning, in which within each cycle the amount of cake removed is slightly less than the amount of new cake formed, was suggested as another potential mechanism. In this case the average filter cake radius slowly expands until cakes on adjacent filters meet.

The development of experimentally verifiable computer models to simulate the gas flow and particle deposits in the filter vessel will provide an important tool for design of future industrial scale filtration systems (Smith & Ahmadi, 1998; Ahmadi & Zhang, 2000; Zhang & Ahmadi, 2001). When filter cakes are the only important deposits, the model of Ferer & Smith (1998), when combined with data such as that obtained by Dahlin et al. (1998) and Kono et al. (1998), gives quantitative answers for the time dependence of the filter cake thickness. When combined with laboratory (Kono et al., 1998; Smith et al., 1997a) and operating data (Smith et al., 1997b), the model of Smith et al. (1998) eventually may be of direct engineering use for solving the problem by improving filter cleaning.

To design reliable hot-gas cleaning filtration systems, a fundamental understanding of particle transport and deposition in the filter vessels is needed. Due to extreme high temperatures and toxicity, direct experimentation of the ash transport during the operation of the industrial-scale filter vessel is not feasible. On the other

hand, computer simulation provides an effective and economical tool for analyzing the transport processes in complex passages. Therefore, computational modeling of gas flow, particle transport, and particle deposition in a filter vessel is a cost-effective technique available for advancing knowledge of the mechanism by which particle deposits begin and grow.

Computer simulations of the hot-gas filtration process were performed by Ahmadi and Smith (1998a). PARTICLE code of Ahmadi and coworkers (Li et al., 1994; He & Ahmadi, 1999) was then used to predict particle deposition patterns. Ahmadi and Smith (1998b) also described a computer simulation study of gas flow and particle deposition in the hot-gas filter vessel at Tidd 70 MWE PFBC Demonstration Power Plant. More recently, Ahmadi and Zhang (2000) and Zhang and Ahmadi (2001) reported a detailed computer simulation of the hot-gas filter vessel at the Power Systems Development Facility (PSDF) in Wilsonville, Alabama, under isothermal conditions.

Temperature variations, however, have been reported in the hot-gas filter vessel at Wilsonville (Guan, 2000) with higher temperatures at the upper portion of the vessel and cooler near the cone. These experimental findings have motivated the present study to include the heat transfer analysis and to improve the previous model of Zhang and Ahmadi (2001). In this study, FLUENT^{TM} computational fluid dynamics software was used to model the nonisothermal gas flows in the filter vessel. The simulation results for gas flow and temperature distribution are presented and discussed. The results for the gas stream pattern show strong rotating flows between the shroud and the refractory liner and in the body of the vessel. The computed temperature distribution in the vessel shows trends that are qualitatively in agreement with the experimental observation at the Power Systems Development Facility.

Power Systems Development Facility

Figure 1 shows the schematics of two advanced coal-fired electricity generating systems. The facility operates in two modes, known as Integrated Gasification Combined Cycle (Figure 1, upper part) and Advanced Pressurized Fluidized Bed Combustors (Figure 1, lower part), that are being tested at the pilot-scale Power Systems Development Facility (PSDF) in Wilsonville, Alabama.

Most U.S coals have moderate to high sulfur content and require addition of a sorbent like limestone to contain in situ SO_x. In the Integrated Gasification Combined Cycle (IGCC) system (Figure 1, upper part) based on the transport reactor, ground coal and limestone are injected into a circulating-transport gasifier/combustor where combustion occurs. The hot gases and entrained fine particles of ash and sulfur pass through a cyclone, which removes large particles. The finer particles that remain are then removed in the filter vessel, so that the cleaning gas can be sent through a fuel cell.

In the Advanced Pressurized Fluidized Bed Combustor (APFBC) system (Figure 1, lower part), coal is introduced into a carbonizer, which converts the coal into char and hot combustible gases. As in the second-generation PFBC, fine particles are removed from the hot gases by a cyclone and filtration unit, the char is fed into a pressurized combustor, and particles are removed from the hot combustor gases by a second cyclone and a filter vessel. The clean gas exiting from the filter vessels is sent through a hot-gas turbine.

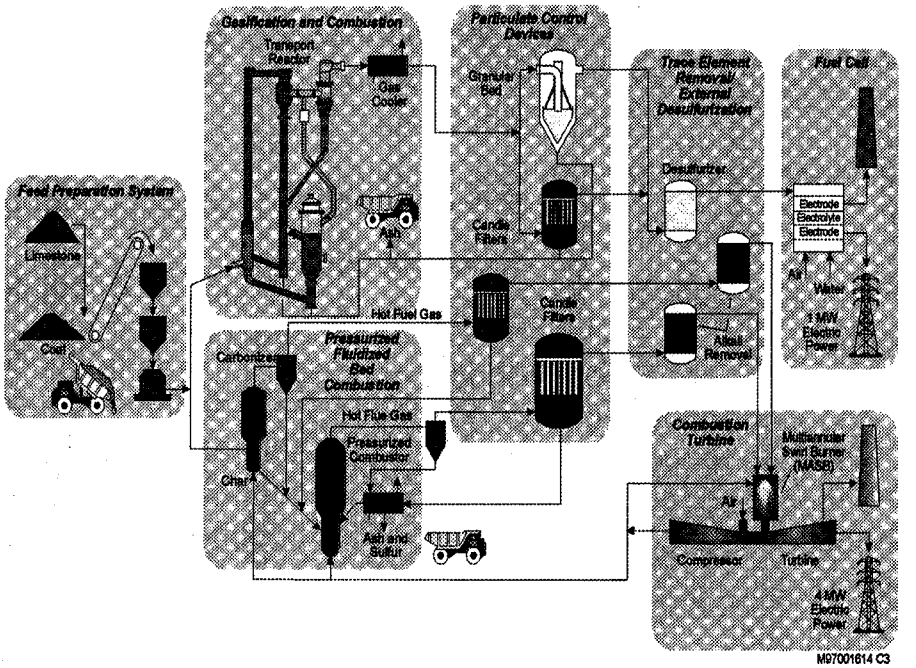

Figure 1. Schematic of the integrated gasification combined cycle (IGCC) and advanced pressurized fluidized bed combustor.

As illustrated in Figure 1, three filter vessels are present at a single site. Here, filtration is performed by cylindrical candle filters, suspended from two plenums inside a pressurized vessel into which the hot gases and suspended particles enter.

Wilsonville Hot-Gas Filter Vessel

A schematic diagram of the Wilsonville filter vessel studied in this paper is shown in Figure 2. Only primary features are illustrated here as the filter has been described in detail by Zhang and Ahmadi (2001).

The vessel accommodates 91 candle filters arranged in two plenums as shown. The upper plenum has 36 and the lower has 55 candle filters. The ceramic candle filters are about 6 cm (2.36 in.) outer diameter and 1.5 m (4.92 ft.) long. The gas enters the vessel tangentially into the shroud. Dust particles are collected on the external surface of the filter, and the dust layer is removed by on-line pulse-jet cleaning of compressed air from inside the filter.

Simulation Conditions

The simulated geometry of the filter vessel showing the outlet and conical region is depicted in Figure 3.

In the present simulations, the group of filters in the upper tier was modeled by six effective cylindrical filters, and the lower cluster of filters was replaced by one effective large cylindrical filter as shown in Figure 4(b). Each one of the effective filters in the upper tier has an outer diameter of 27.94 cm (11 in.) and an inner

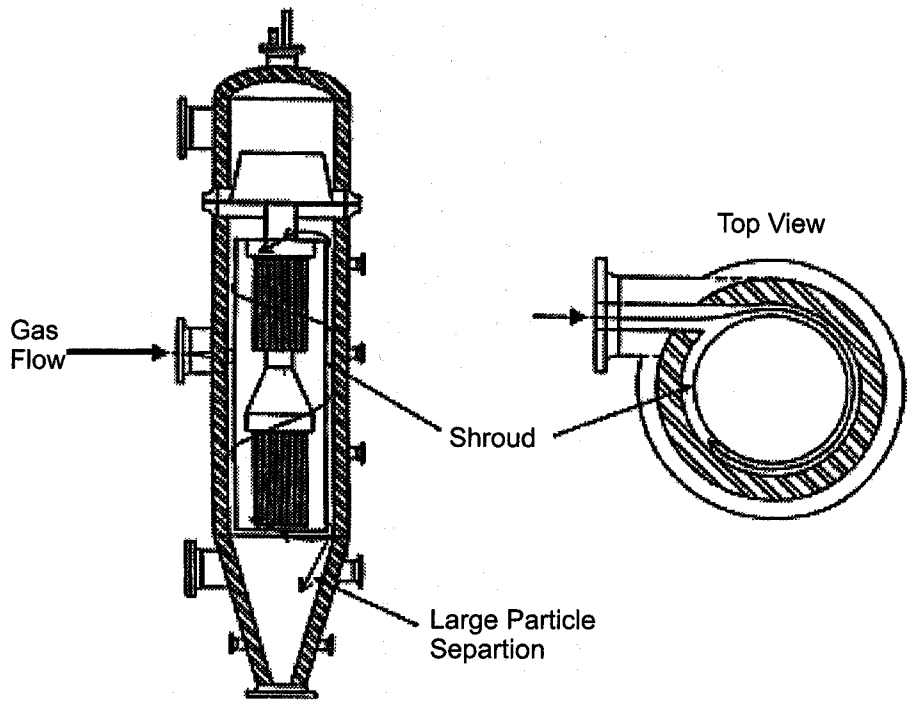

Figure 2. Schematic of the Wilsonville filter vessel.

diameter of 23.88 cm (9.4 in.), while the outer diameter of the lower filter is 96.01 cm (37.8 in.) and its inner diameter is 40.64 cm (16 in.). The effective permeability of the effective filters was estimated so that they have the same pressure drop and the same face velocities as the actual candle filters. The permeabilities for the upper and lower equivalent filters are, respectively, 9×10^{-13} and $2 \times 10^{-11}\,m^2$. The gas at 760°C (1033 K) enters the vessel tangentially into the shroud with a superficial velocity of 9.815 m/s and turbulence intensity of 5%. The air density, viscosity, and heat capacity were, respectively, 4.53 kg/m^3, 3.7×10^{-5} kg/m.s, and 1006.4 J/kg K. The operating pressure was 1344 kPa.

Model

The gas flow in the filter vessel is in a state of turbulence motion. It is, therefore, important to use an appropriate turbulence model for evaluating the mean flow field. The FLUENT^{TM} code provides options for using either the k-ε standard version or the Reynolds Stress Transport Model (RSTM). While the k-ε model is widely used in industrial applications, it suffers from several shortcomings. Its use of an isotropic eddy viscosity limits its applicability and causes the model to be incapable of handling the turbulence normal stress effects. The RSTM, on the other hand, accounts for the evolution of individual turbulent stress components. Therefore, the RSTM entirely avoids the use of an eddy viscosity and is clearly well suited for handling anisotropic turbulence fluctuations. Following the work of Ahmadi and Smith (1998a, 1998b) and Zhang and Ahmadi (2001), the RSTM is used in this study.

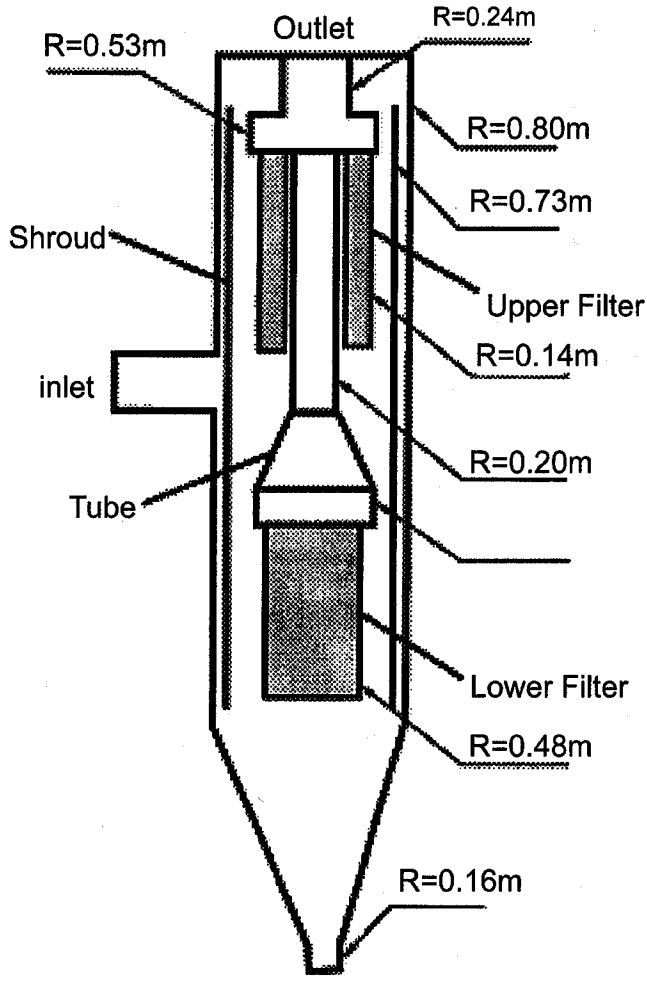

Figure 3. The model of the Hot-gas filter Vessel: the dimensions of the vessel geometry.

For an incompressible fluid, the equations for the conservation of mass and momentum for the mean motion are given as

$$\frac{\partial \bar{u}_i}{\partial x_i} = 0, \tag{1}$$

$$\frac{\partial \bar{u}_i}{\partial t} + \bar{u}_j \frac{\partial \bar{u}_i}{\partial x_j} = -\frac{1}{\rho}\frac{\partial \bar{p}}{\partial x_i} + \vartheta \frac{\partial^2 \bar{u}_i}{\partial x_j^2} - \frac{\partial R_{ij}}{\partial x_j}, \tag{2}$$

where $\bar{u}_i$ is the mean velocity, x_i is the position, t is the time, $\bar{p}$ is the mean pressure, ρ is the constant mass density, ϑ is the kinematic viscosity, and $R_{ij} = \overline{u_i' u_j'}$ is the Reynolds stress tensor. Here, $u_i' = u_i - \bar{u}_i$ is the fluid fluctuation velocity.

The Reynolds Stress Transport Model (RSTM) provides for differential transport equations for evaluation of the turbulence stress components, i.e.,

$$\frac{\partial R_{ij}}{\partial t} + \bar{u}_k \frac{\partial R_{ij}}{\partial x_k} = \frac{\partial}{\partial x_k}\left(\frac{\nu_t}{\sigma^k}\frac{\partial R_{ij}}{\partial x_k}\right) - \left[R_{ik}\frac{\partial \bar{u}_j}{\partial x_k} + R_{jk}\frac{\partial \bar{u}_i}{\partial x_k}\right] - C_1\frac{\varepsilon}{k}\left[R_{ij} - \frac{2}{3}\delta_{ij}k\right] - C_2\left[P_{ij} - \frac{2}{3}\delta_{ij}P\right] - \frac{2}{3}\delta_{ij}\varepsilon, \tag{3}$$

where the turbulence production terms are defined as

$$P_{ij} = -R_{ik}\frac{\partial \bar{u}_j}{\partial x_k} - R_{jk}\frac{\partial \bar{u}_i}{\partial x_k}, \quad P = \frac{1}{2}P_{kk}, \tag{4}$$

with P being the fluctuation kinetic energy production. Here $\sigma^k = 1.0, C_1 = 1.8$, and $C_2 = 0.6$ are empirical constants (Launder et al., 1975).

The transport equation for the turbulence dissipation rate ε is given as

$$\frac{\partial \varepsilon}{\partial t} + \bar{u}_j\frac{\partial \varepsilon}{\partial x_j} = \frac{\partial}{\partial x_j}\left[\left(\vartheta + \frac{\nu t}{\sigma^\varepsilon}\right)\frac{\partial \varepsilon}{\partial x_j}\right] - C^{\varepsilon 1}\frac{\varepsilon}{k}R_{ij}\frac{\partial \bar{u}_i}{\partial x_j} - C^{\varepsilon 2}\frac{\varepsilon^2}{k}. \tag{5}$$

In Equation (5), $k = \frac{1}{2}\overline{u_i' u_i'}$ is the turbulence kinetic energy, and ν_t is the "eddy" or turbulent viscosity. The values of constants are

$$\sigma^\varepsilon = 1.3, C^{\varepsilon 1} = 1.44, C^{\varepsilon 2} = 1.92. \tag{6}$$

The RSTM of the FLUENT^{TM} code and the standard wall function boundary condition were used for evaluating the mean velocity field and the Reynolds stresses in the filter vessel.

For the energy transport equation, we solved the convection-diffusion heat transfer equation given as

$$\frac{\partial \bar{T}}{\partial t} + \bar{u}_j\frac{\partial \bar{T}}{\partial x_j} = \frac{\partial}{\partial x_j}\left[\left(\alpha + \frac{\nu_t}{\sigma^T}\right)\frac{\partial \bar{T}}{\partial x_j}\right]. \tag{7}$$

Here $\bar{T}$ is the mean temperature, α is the thermal conductivity, and σ^T is the temperature turbulent Prandtl number.

In the solution procedure, we assume that the flow and heat transfer equations are decoupled, i.e., the properties are temperature-independent and the buoyancy force is negligible. Previous preliminary simulation studies, conducted during this study, have shown that although the temperature variation is in the order of several hundred degrees, the variation of the fluid properties is not significant, and the average constant values are used for the gas properties. Based on the decoupling assumption, we first solved the isothermal flow and obtained a converged flow field solution, and then solved the energy transport equation to find the temperature variation in the vessel.

Results and Discussion

Figure 4 shows the unstructured grid of about 3000 points generated by the GAMBIT software package used in this study to mesh the model.

Figure 4(a) shows the surface grid and Figure 4(b) shows the grid for the inner structure of the vessel. This figure displays the inlet, outlet, shroud, tube sheets, the effective upper and lower cylindrical filters, and the connecting post.

As stated before, the Reynolds stress transport turbulence model and the heat transfer equation were used in these computations. In the simulation, the origin of the coordinate system is set in the center of the circle on top of the vessel. The z-axis is in the vertical direction (gravitational direction) and the x-axis is along the inlet flow direction. An essentially grid independent solution was demonstrated. Figure 5 shows the gas temperature variation in the vessel. It is observed that the temperature is higher at the inlet (1033 K), cooler near the conical section, and higher at the outlet. Unfortunately, quantitative data for comparison are not available at the present time, generally higher temperature in the upper part of the vessel when compared with its lower part is observed experimentally (Guan, 2000), and this trend is predicted by the present model.

The contour plots for gas temperature gradients in various planes are shown in Figure 6. This figure confirms that the temperature is higher in the upper part of the filter vessel than in the lower part.

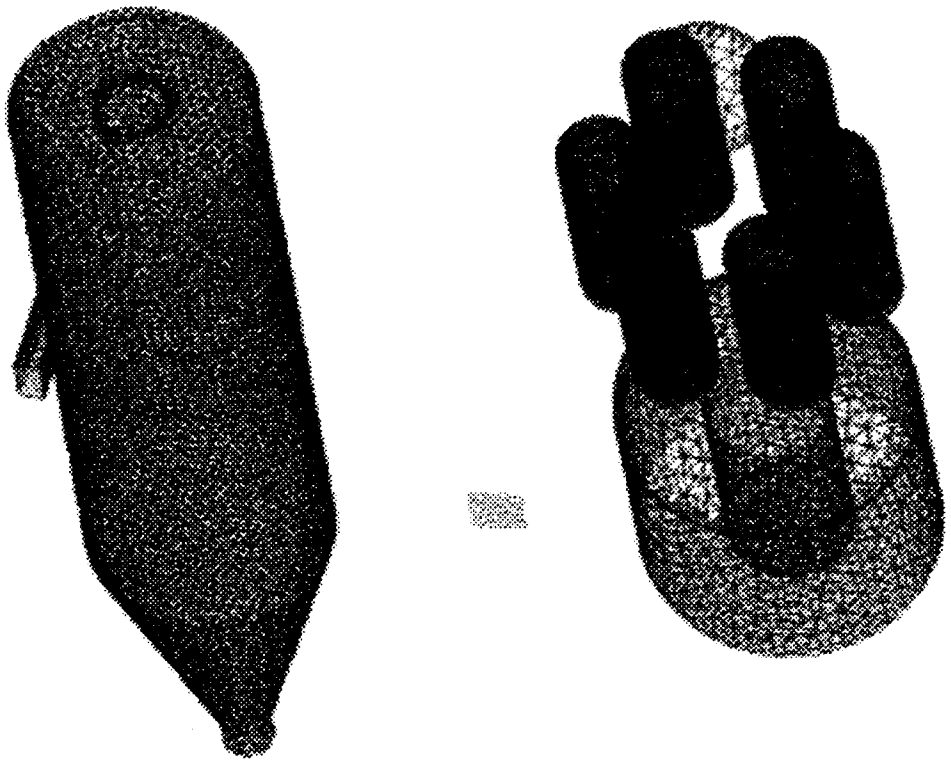

Figure 4. The computational grid for the filter vessel. (a) outer shell; (b) internal structures.

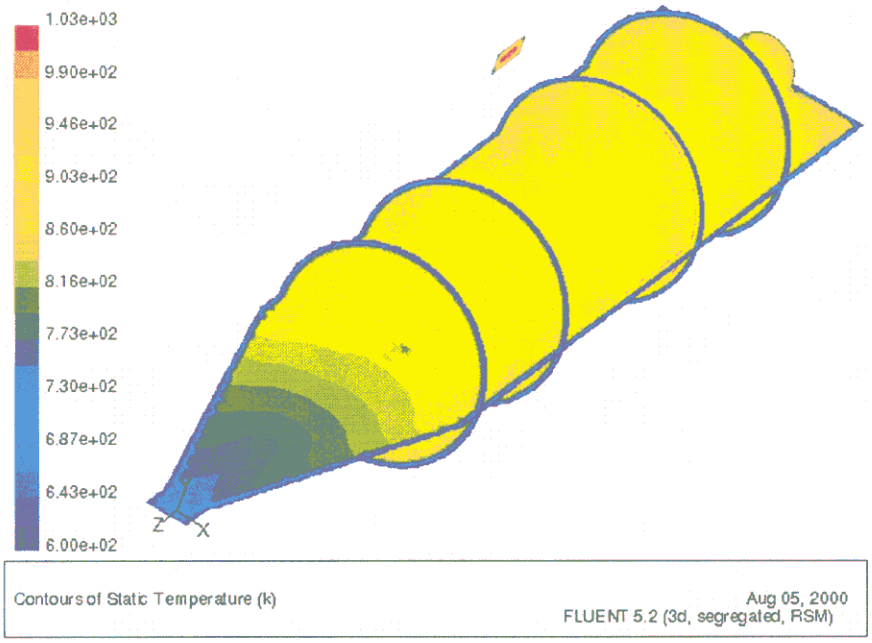

Figure 5. Gas temperature contours in the filter vessel.

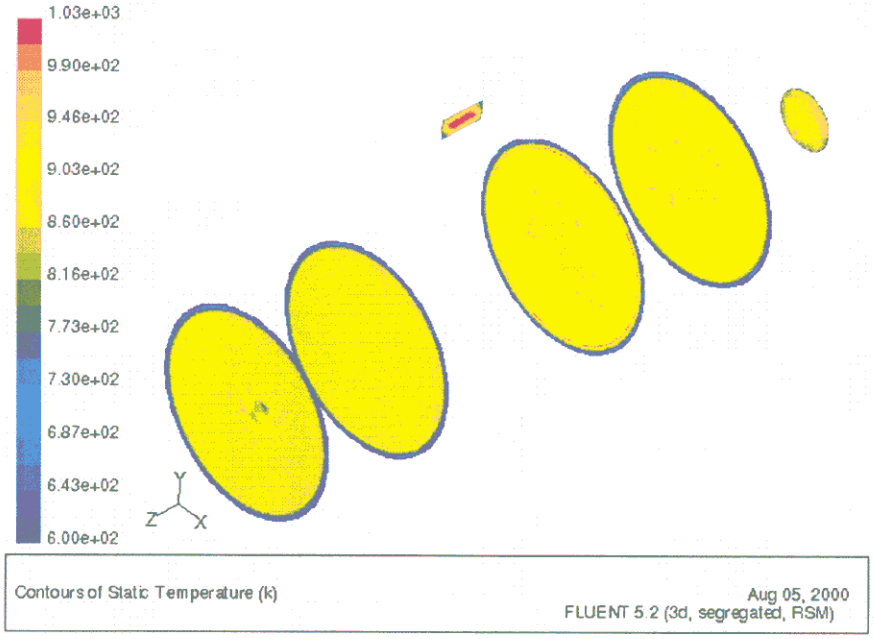

Figure 6. Gas temperature contours at different sections in the filter vessel.

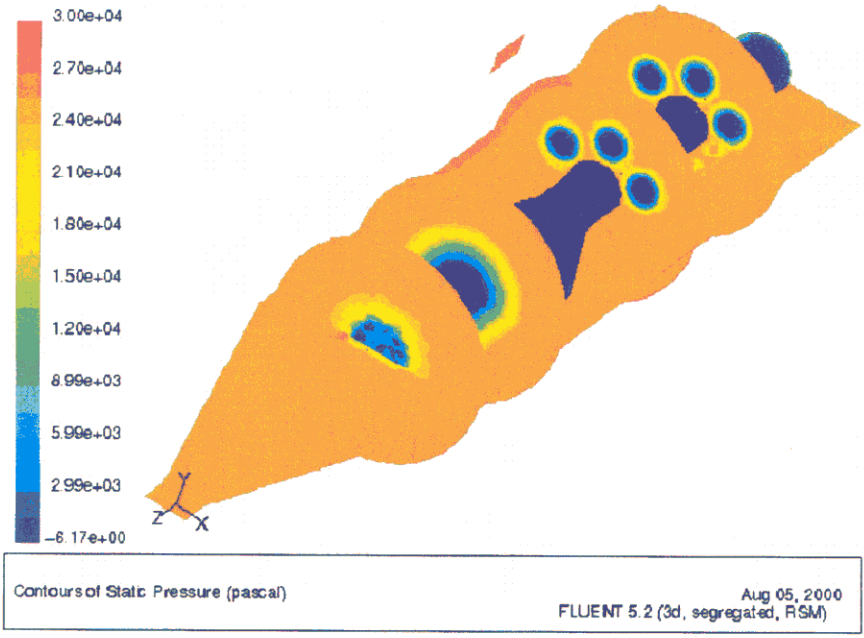

Figure 7. Gas pressure contours in the filter vessel.

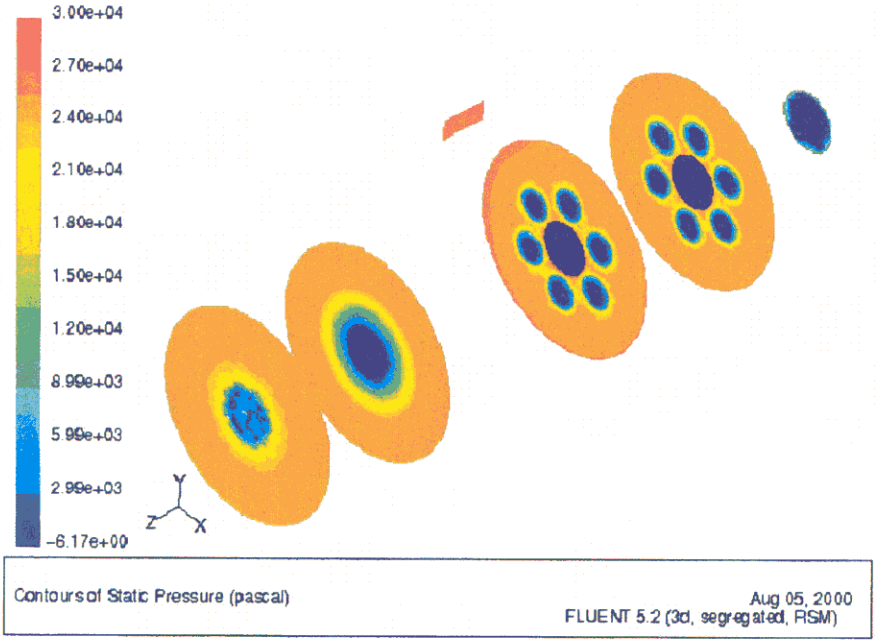

Figure 8. Gas pressure contours at different sections in the filter vessel.

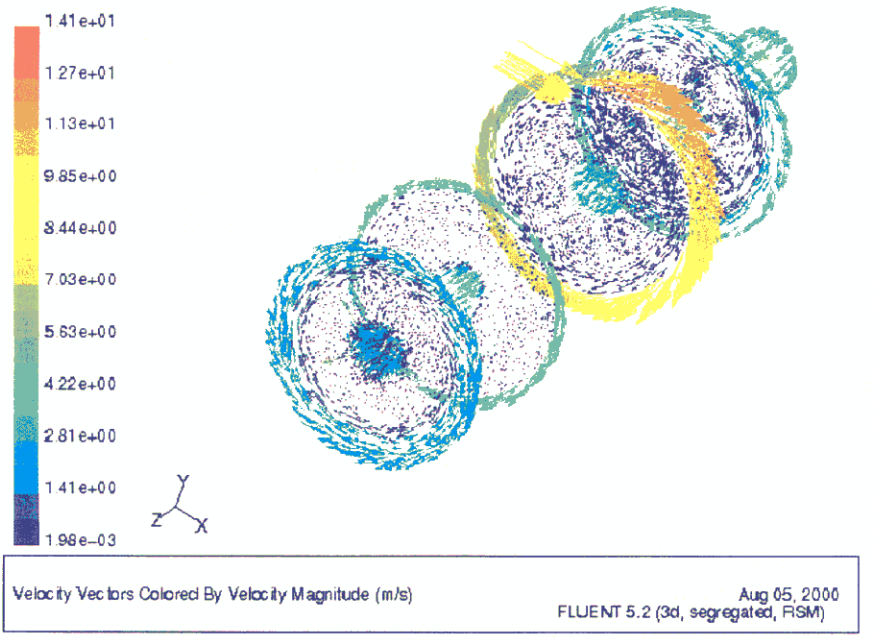

Figure 9. Velocity vector field in a plane across the filter vessel.

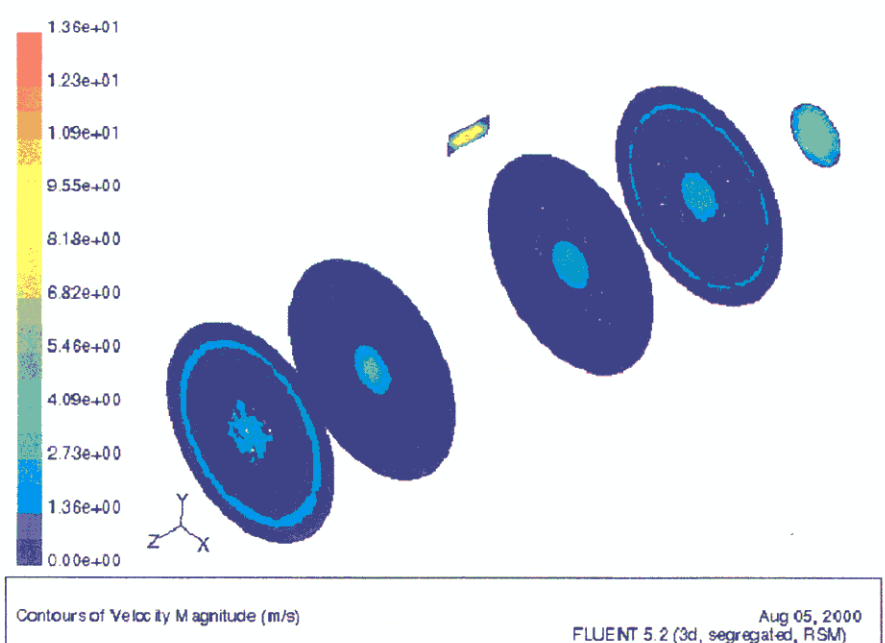

Figure 10. Velocity magnitude contour in the filter vessel.

The contour plots for variations of the static pressure are shown in Figure 7. This figure shows that the pressure is roughly uniform inside the filter vessel (about 25 kPa).

Figure 8 shows the static pressure at different cross-sectional areas. This figure shows that the main pressure drop occurs across the candle filter walls and that the pressure reduces to about 29 kPa inside the filter cavity. The air pressure inside the filter cavity and connecting pipes is roughly constant with a slight decrease toward the vessel outlet. This observation is consistent with the earlier results of Zhang and Ahmadi (2001).

The velocity vector fields in a plane across the filter vessel are shown in Figure 9. This figure shows that a strong rotating flow region occurs outside the shroud and inside the filter vessel near the upper and lower parts. It is also observed from Figure 9 that the velocity is quite low inside the vessel.

The velocity magnitude contour in Figure 10 shows that the velocity is quite high at the inlet but becomes quite low in the body of the vessel. The velocity magnitude increases in the outlet pipe as the gas leaves the vessel.

Conclusions

This study was undertaken to assess the gas temperature distribution in the Wilsonville filter vessel. The energy transport equation was used with the Reynolds stress transport turbulence model to simulate the gas flows in the Wilsonville filter vessel. The simulated gas temperature distributions in the vessel qualitatively agree with the experimental findings, showing nonisothermal conditions with higher temperature in the upper part of the filter and lower temperature near the cone. Strong rotating flow regions were also predicted inside the filter vessel near the upper and lower parts, which are also in agreement with the field observations. The pressure was found to be roughly uniform inside the filter vessel and the main pressure drop occurring across the candle filter vessel walls.

Successful development of computational fluid dynamic models for hot-gas filter vessels, similar to the model described in this study, is needed to provide a tool for the design of new systems, scale-up of laboratory scale models, and efficient operation of filter vessels. Consequently, the production of electricity from coal in an environmentally acceptable manner will proceed at a more efficient pace.

Nomenclature

k	turbulence kinetic energy
p	gas pressure
P	fluctuating kinetic energy production
R_{ij}	Reynolds stress tensor
t	time
T	gas temperature
u_i	gas velocity vector
u_i'	gas fluctuating velocity vector
x	position

Greek letters

α	thermal conductivity
δ_{ij}	unit tensor

ε rate of dissipation of kinetic energy of turbulence
ϑ kinematic viscosity
ν viscosity
ρ mass density
σ turbulent Prandtl number

Subscripts

t turbulent (prefix)
i, j = x, y, z

Superscripts

k for turbulence kinetic energy
T for temperature
ε for rate of dissipation of kinetic energy of turbulence
- mean

References

Ahmadi, G., & D. H. Smith 1998a. Particle transport and deposition in a hot-gas cleanup pilot plant, *Aerosol Sci. Technol.* 29: 183–205.

Ahmadi, G., & D. H. Smith 1998b. Gas flow and particle deposition in the hot-gas filter vessel at the Tidd 70 MWE PFBC Demonstration Power Plant. *Aerosol Sci. Technol.* 29: 206–223.

Ahmadi, G., & H. Zhang 2000. Hot-gas flow and particle transport and deposition in the filter vessel at Wilsonville. *Proceedings of Seventeenth Annual International Pittsburgh Coal Conference, Pittsburgh, PA, September 11–14.*

Dahlin, R. S., E. C. Lendham, & H. L. Hendrix. 1998. In situ particulate sampling and ash characterization at the Power Systems Development Facility. *Aerosol Sci. Technol.* 29: 170–182.

Ferer, M., & D. H. Smith 1998. Modeling of filter cleaning: the small-particle filter-cake fragments. *Aerosol Sci. Technol.* 29: 246–256.

Guan, X. 2000. Personal communication. July 26.

He, C., & G. Ahmadi 1999. Particle deposition in a nearly developed turbulent duct flow with electrophoresis. *J. Aerosol Sci.* 30: 793–758.

Kono, H. O., L. M. Richman, B. R. Jordan, & D. H. Smith 1998. Filter-cake property characterization for hot gas candle filters. *Aerosol Sci. Technol.* 29: 236–245.

Launder, B. E., G. J. Reece, & W. Rodi 1975. Progress in the development of a Reynolds stress turbulence closure. *J. Fluid Mech.*, 68: 537–566.

Li, A., G. Ahmadi, R. G. Bayer, & M. A. Gaynes 1994. Aerosol particle deposition in an obstructed turbulent duct flow. *J. Aerosol Sci.* 25: 91–112.

Lippert, T. E., G. J. Bruck, Z. N. Sanjana, & R. A. Newby. 1995. Westinghouse advanced particle filter system. *Proceedings of Advanced Coal-Fired Power System '95, Review Meeting, Morgantown, WV, June 27–29*, DOE/METC-95/10108, 123–139.

Radian Corporation, 1994. *A Study of Hazardous Air Pollutants at the Tidd PFBC Demonstration Plant*, DCN 94-633-021-03. Morgantown, WV: Morgantown Energy Technology Center.

Smith, D. H., & G. Ahmadi 1998. Problems and progress in hot-gas filtration for pressurized fluidized bed combustion (PFBC) and integrated gasification combined cycle (IGCC). *Aerosol Sci. Technol.* 29: 224–235.

Smith, D. H., G. J. Haddad, & U. Grimm 1997a. Composition and chemistry of particulates from a PFBC demonstration plant. *Fuel.* 76: 727–732.

Smith, D. H., G. J. Haddad, & M. Ferer 1997b. Shear strengths of heated and unheated mixtures of $MgSO_4$ and $CaSO_4$ powders: Model pressurized fluidized bed combustion filter cakes. *Energy Fuels.* 11: 1006–1011.

Smith, D. H., V. Powell, G. Ahmadi, & M. Ferer 1998. Analysis of operational filtration data, Part III: Re-entrainment and incomplete cleaning of dust cake. *Aerosol Sci. Technol.* 29: 224–235.

Zhang, H., & G. Ahmadi 2001. Particle transport and deposition in the hot-gas filter vessel at Wilsonville. *Powder Technol.* 116: 53–68.